THE ASTROPHYSICAL JOURNAL, 481:452–466, 1997 May 20

ABUNDANCE ANALYSES OF FIELD RV TAURI VARIABLES. III. DY AQUILAE, SS GEMINORUM, CT ORIONIS, AND CE VIRGINIS

GUILLERMO GONZALEZ
Astronomy Department, University of Washington, Seattle, WA 98195; gonzalez@astro.washington.edu
DAVID L. LAMBERT
Department of Astronomy, University of Texas, Austin, TX 78712; dll@astro.as.utexas.edu
AND
SUNATRA GIRIDHAR
Indian Institute of Astrophysics, Bangalore, 560 034 India; giridhar@iiap.ernet.in
Received 1996 October 7; accepted 1996 December 11

ABSTRACT

Analyses of the photospheric compositions of the four field RV Tauri stars, DY Aql, SS Gem, CT Ori, and CE Vir, indicate that to varying degrees they have experienced fractionation processes that have preferentially depleted their atmospheres of elements with high condensation temperatures. This corroborates our previous studies, which showed similar patterns in five other field RV Tauri stars.

Two stars in our sample, DY Aql and CE Vir, were found to have strong Li I resonance lines, with corresponding lithium abundances near log $\epsilon(\text{Li}) = 0.0$; this is not significantly different from that found in less evolved M giants. These are also the coolest stars displaying a correlation of photospheric abundances with condensation temperatures.

Subject headings: stars: abundances — stars: late-type — stars: variables: other (RV Tauri)

1. INTRODUCTION

This is the third in a series of studies concerning the chemical composition of field RV Tauri variables. Giridhar, Rao, & Lambert (1994, hereafter Paper I) and Gonzalez, Lambert, & Giridhar (1996, hereafter Paper II) performed detailed abundance analyses of five field RV Tauri stars. Their results indicated the presence of abundance patterns distinct from either disk or halo stars; most elements have abundances between one and two dex below the solar values, but the abundances of C, N, O, S, and Zn are similar to disk stars. In Papers I and II we have shown that the abundances of the elements correlate with their condensation temperatures, where the condensation temperature of a given element is that temperature at which half the atoms in a gaseous environment condense out of the gas phase. It is presumed that the present photosphere consists of gas from which elements of high condensation temperature have been removed as dust grains. In Papers I and II we suggested that the gas-dust separation occurs in the circumstellar shell. The correlation of abundance with condensation temperature is also seen in the interstellar medium, where it is assumed that the elements with the highest condensation temperatures have condensed onto grains. In order to better understand the phenomenon causing this pattern among the RV Tauri stars, it is helpful to sample as much parameter space (effective temperature, luminosity, metallicity, binarity, etc.) as possible. To help further this end we have selected four additional field RV Tauri variables: DY Aql, SS Gem, CT Ori, CE Vir. Their general characteristics are given in Table 1.

DY Aql and CE Vir are cooler than the average RV Tauri star; Wahlgren (1992) assigned a spectral type of K5 to DY Aql based on eight-color photometry. While the status of CE Vir as an RV Tauri star is not certain (Dawson 1979 lists it as an SRd star), we included it because of its spectroscopic similarity to DY Aql (classified as an RV Tauri star by Preston et al. 1963 and studied in some detail by Wahlgren). These two RV Tauri stars are also unusual in that they have higher than average heights above the Galactic disk compared to other members of their class.

In Papers I and II we showed that the high condensation temperature elements are strongly depleted in Preston group B RV Tauri stars (C-rich, metal-poor). We now know that the large C abundance relative to Fe in these stars is most likely due to a depletion of Fe rather than an enhancement of C. In order to further test the hypothesis that all group B RV Tauri stars are depleted, we have included SS Gem and CT Ori, both group B objects, in the present study.[1]

2. OBSERVATIONS

Spectra were obtained between 1993 December and 1996 April with the McDonald Observatory 2.1 m telescope equipped with a Cassegrain echelle spectrograph and a Reticon 1200 × 400 pixel CCD (McCarthy et al. 1993). In addition, a spectrum of CE Vir was obtained with the coude cross-dispersed echelle (Tull et al. 1995) on the 2.7 m telescope at McDonald Observatory on 1996 July 19; the resolving power of this instrument is about 60,000. The typical resolving power of the 2.1 m spectra as measured from the Th-Ar comparison spectra is about 45,000. Sample reduced spectra are presented in Figure 1. The data reduction procedures are described in Paper II.

The S/N ratios average near 140 for DY Aql, 200 for SS Gem, 150 for CT Ori, and 170 for CE Vir, which are sufficiently high to perform accurate abundance analyses on each of these stars. Many more spectra of DY Aql, CT Ori, and CE Vir were obtained than used in the final analysis. Most of the spectra of DY Aql and CE Vir were rejected due

[1] Preston et al. (1963) originally classified SS Gem as belonging to spectroscopic group A. Since then it has been quoted as an RVA star in published literature. We claim that it should be reclassified as a group B star based on the numerous C I lines in its spectrum.

TABLE 1

BASIC PARAMETERS OF THE PROGRAM STARS

Parameter	DY Aql	SS Gem	CT Ori	CE Vir
V^a	~9.8–11.3	8.6–9.4	9.1–11.0	~ 8.7–10.7
$B-V^a$	~1.17–1.75	0.77–1.42	0.85–1.24	~0.89–1.43
$E(B-V)^b$	0.14	0.56	0.52	0.03
Spectral type[c]	G8e–M3 Ia	F8–G0	F9	G–K
$\langle T_{eff} \rangle^d$	4250	5400	5700	4300
Period (days)	131.4	89.2	135.5	85?
Galactic latitude (deg)	−17.1	1.3	−4.6	57.8
$\|z\|$ kpc[e]	0.9	0.0	0.3	1.7
IR excess?[f]	no	yes	yes	?
Spectroscopic group[g]	A	B	B	A?
Photometric type[g]	?	RVa	?	?

[a] Sources of apparent V, $B-V$ magnitudes are: DY Aql, Dupuy 1973 and Goldsmith et al. 1987; SS Gem, Zsoldos 1991; CT Ori, Dawson 1979; CE Vir, Dawson 1979 and Dawson & Patterson 1982. The photometric data available for DY Aql, CT Ori, and CE Vir are fragmentary.

[b] $E(B-V)$ was estimated for SS Gem and CT Ori using the charts of Neckel & Klare 1980. The estimate for DY Aql and CE Vir are based on the H I maps of Burstein & Heiles 1982.

[c] Spectral types are from Preston et al. 1963 for DY Aql and SS Gem and from the GCVS for CT Ori and CE Vir.

[d] Mean temperature estimates are based on our Fe-line analysis and the photometry. Values are given in degrees K.

[e] The height above the Galactic plane was estimated using the period-luminosity relation of Gonzalez 1994 assuming fundamental mode pulsation, mass = 0.5 $M_\odot$, and mean temperatures.

[f] These are stars for which a significant flux has been measured by *IRAS* (Raveendran 1989).

[g] The spectroscopic groups are those defined by Preston et al. 1963. The photometric types are based on long-term photometric behavior.

to the presence of strong TiO bands, mostly in the red spectral regions. Weak line asymmetries are evident on the spectra of CE Vir (contributing about 10% to the total W_λ of a line); the W_λ estimate of an asymmetric line has been determined by fitting a Gaussian function to the main component so as to exclude the asymmetric portion. This must result in a slight underestimate of the abundances for this star, but the relative abundances should be unaffected. Several spectra of CT Ori were rejected due to the presence of strong Hα or Hβ emission, which are indicative of a disturbance in the atmosphere produced by the passage of a shock. The typical uncertainty of an W_λ measurement of a moderate strength line is ± 3–6 mÅ for DY Aql, ± 1–3 mÅ for SS Gem, 2–4 mÅ for CT Ori, and ± 3–5 mÅ for CE Vir spectra. These uncertainties were reduced in those cases where a running average was applied to unblended lines, which was most often done for the spectra CT Ori.

3. ABUNDANCE ANALYSIS

3.1. *Model Atmosphere Selection and* Fe *Abundance*

As in Papers I and II the stellar atmospheric parameters are determined from Fe I and Fe II lines. The *gf*-values of Fe I are primarily from Lambert et al. (1996); a few are from Nave et al. (1994) and Gonzalez & Lambert (1996); the *gf*-values for most of the other elements are from a database of laboratory determinations maintained by R. E. Luck at Case Western Reserve University (private communication). It was not possible to use the same lines for each star given the large range in effective temperature, T_{eff}, and metallicity they span. As in Paper II spectra obtained on consecutive nights were combined. The adopted atmospheric parameters and Fe abundances for each spectrum are given in Table 2.

The uncertainties in T_{eff} are typically ± 150 K, except the 1994 March 2 and 3 spectra of SS Gem, which is ± 250 K, the 1994 June 24 spectrum of DY Aql, which is ± 200 K, and the 1996 July 19 spectrum of CE Vir, which is ± 100 K. The typical uncertainty in the log g estimates is ± 0.2 (cgs), except those spectra with large uncertainties in the Fe II abundance, where it is about ± 0.5. The uncertainties in the microturbulence parameter, ξ_t, are about ± 0.2–0.3 km s^{-1}. These uncertainties in the atmospheric parameters, combined with the line-to-line scatter and the sensitivities to changes in atmospheric parameters tabulated in Table 4 of Paper II, lead to typical uncertainties in [Fe/H] near ± 0.10 dex.

The individual Fe I and Fe II line abundances of DY Aql, SS Gem, CT Ori, and CE Vir are given in Tables 3, 4, 5, and 6, respectively. The average values of [Fe/H] are listed in Table 7. The results of the abundance analysis for DY Aql are less reliable than for the other three stars, since they are based on only one spectrum.

3.2. Li *in DY Aql and CE Vir*

The resonance Li I doublet at 6707.8 Å is strong in the spectra of DY Aql and CE Vir; the values of W_λ are about 300 mÅ for the spectrum of DY Aql and 230 mÅ for the 1996 April 9 spectrum of CE Vir. We compare the spectral region containing the Li I line in Figure 2 between DY Aql and SS Gem, which differ in temperature by 500 K. The region between 6702 and 6710 Å was synthesized using the line list of Cunha, Smith, & Lambert (1995) with the model atmosphere parameters listed in Table 2. The first attempt at synthesizing the Li I line in the spectra of CE Vir revealed that the Li I line width is greater than can be accounted for by the Li I doublet alone. There are two possible solutions to this problem: the presence of a significant contribution from ^{6}Li or the distortion of the line by another velocity component of the ^{7}Li doublet.

The first possibility was tested by including ^{6}Li

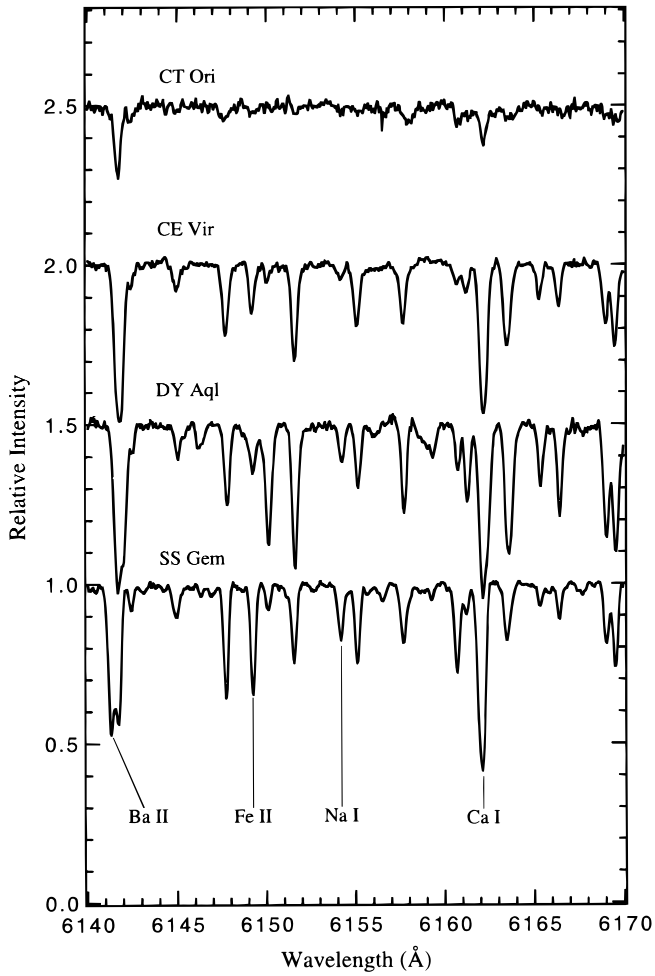

FIG. 1.—Sample spectra of the program stars. The spectra have been shifted to the rest frame, normalized to the continuum, and shifted vertically. These samples are from 1994 January 20, 1994 June 24, 1996 April 9, and 1996 April 9 for SS Gem, DY Aql, CE Vir, and CT Ori, respectively.

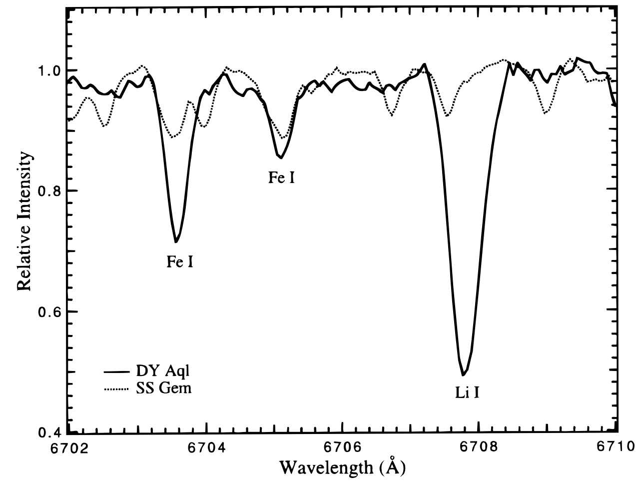

FIG. 2.—Spectral region containing the Li I resonance line. Shown are the spectra of DY Aql from 1994 June 24 and SS Gem from 1994 January 20. Most of the unlabeled weak lines in the spectrum of SS Gem are due to CN.

(wavelengths obtained from Smith, Lambert, & Nissen 1993) in the synthesis and adjusting the isotopic ratio until the best fit was obtained. The resulting isotopic ratio, ^{6}Li/^{7}Li, for the 1996 April 9 spectrum is about 0.52, with a close match between the synthetic and observed profiles. The second possibility can be tested by comparing the Li I line profile to that of resonance K I line at 7699 Å, which, also being an alkali metal, behaves in a similar way. The only spectrum containing both the Li I and the K I lines is the one obtained on 1996 July 19. Syntheses of the lines on this spectrum indicates that the asymmetry is also present in the K I line and that its magnitude is similar to that of the Li I line. Inspection of the resonance Na I lines also indicates the presence of an asymmetry. Hence, while the presence of some ^{6}Li cannot be ruled out, the most likely explanation

TABLE 2

STELLAR PARAMETERS OF THE RV TAURI STARS DERIVED FROM THE Fe-LINE ANALYSES

UT Date	Model ($T_{\rm eff}$, log g, [Fe/H])	ξ (km s^{-1})	Fe I log ϵ	N	Fe II log ϵ	N	Comments
			DY Aql				
1994 Jun 24	4250, 0.6, −1.0	3.3	6.47 ± 0.05	13	6.45 ± 0.10	3	Weak TiO, strong Li I
			SS Gem				
1993 Dec 6	5500, 0.2, −1.0	3.1	6.54 ± 0.02	32	6.54 ± 0.03	6	
1994 Jan 20	4750, −0.2, −1.0	3.5	6.52 ± 0.02	13	6.51 ± 0.07	3	Weak Hα emission, weak CN
1994 Mar 2, 3	6500, 0.5, −1.0	2.4	6.84 ± 0.03	15	6.82 ± 0.05	4	Weak Hα emission, no Hγ emission
			CT Ori				
1995 Dec 10, 11	5500, 1.0, −2.0	2.0	5.61 ± 0.03	19	5.62 ± 0.16	4	Moderate Hα emission
1996 Apr 9, 10	6000, 1.0, −2.0	2.6	5.65 ± 0.02	22	5.64 ± 0.01	3	Moderate/strong Hα, weak Hβ emission
			CE Vir				
1994 Jan 20	4250, 0.0, −1.0	2.8	6.26 ± 0.03	13	6.24 ± 0.16	3	Weak TiO, strong Li I
1995 Jan 24	4500, 0.8, −1.0	3.5	6.36 ± 0.02	14	6.38 ± 0.15	2	Weak TiO, strong Li I
1996 Apr 9	4500, 0.7, −1.0	3.5	6.32 ± 0.02	21	6.32 ± 0.10	4	No molecular bands, strong Li I
1996 Jul 19	4250, −0.2, −1.0	2.6	6.30 ± 0.02	19	6.30 ± 0.03	3	No molecular bands, strong Li I

NOTE.— log ϵ is the mean number density abundance relative to H (with log $N_{\rm H}$ = 12.00); the solar value of log ϵ(Fe) is 7.50. Also listed are the standard deviations of the means, calculated from the line-to-line scatter.

TABLE 3

INDIVIDUAL ABUNDANCE RESULTS FOR DY AQUILAE USING THE MODEL ATMOSPHERE LISTED IN TABLE 2

Wavelength (Å)	Low E.P. (eV)	log gf	W_λ (mÅ), log ϵ (1994 Jun 24)
	Li I		
6707.8	0.00	0.17	SS, 0.05
	Na I		
6154.23......	2.10	−1.57	47, 5.61
	Si I		
6125.03......	5.61	−1.51	32, 6.97
	Ca I		
6166.44......	2.52	−1.14	92, 5.29
6471.67......	2.52	−0.69	160, 5.44
	Sc II		
6604.60......	1.36	−1.53	28, 1.64
	Fe I		
5809.22......	3.88	−1.69	84, 6.62
5852.22......	4.55	−1.18	82, 6.92
6027.05......	4.08	−1.09	112, 6.51
6056.01......	4.73	−0.40	89, 6.42
6079.01......	4.65	−0.97	58, 6.58
6151.62......	2.18	−3.29	182, 6.90
6165.36......	4.14	−1.47	67, 6.53
6200.31......	2.61	−2.44	163, 6.43
6469.12......	4.84	−0.62	105, 6.91
6703.55......	2.76	−3.05	109, 6.70
6733.15......	4.64	−1.43	36, 6.71
6806.84......	2.73	−3.13	119, 6.81
6820.37......	4.64	−1.17	61, 6.76
	Fe II		
6084.10......	3.20	−3.80	50, 6.85
6369.46......	2.89	−4.19	37, 6.67
6432.28......	2.89	−3.58	70, 6.50
	Co I		
6116.99......	1.79	−2.49	76, 4.54
	Ni I		
6111.06......	4.09	−0.87	40, 5.35
	Eu II		
6645.13......	1.38	0.20	40, −0.05

NOTE.—The gf-value of lithium is from Anderson et al. 1984. SS is an abbreviation for spectrum synthesis.

for the Li I line asymmetry is an additional velocity component.

3.3. *Other Elements*

Absorption lines of 19 elements in addition to Fe were carefully selected for use in abundance estimates. The selection criteria are similar to those employed in Paper II. We list the W_λ and abundance estimates in Tables 3–6. The abundances were calculated using the model atmosphere parameters derived from the Fe-line analysis (Table 2). The final average abundance for each element are listed in Table 7. The uncertainties of the [X/H]-values were estimated using the data in Table 4 of Paper II. The solar abundances are also listed in Table 7; they were calculated from some of the same lines used in the present analysis (measured on the Solar Flux Atlas; Kurucz et al. 1984) using the same gf-values. Hyperfine line structure was not included in any of the abundance estimates (for a discussion of the effects of neglecting the hyperfine effect, see Gonzalez & Wallerstein 1994).

4. DISCUSSION

4.1. *Abundance Patterns*

The present results are similar to those reported in Papers I and II; the abundances of C, O, S, and Zn are high relative to the other elements. This is further evidence of preferential depletion of elements with high values of $T_{\rm cond}$; all four stars display some correlation (Fig. 3), the clearest being SS Gem and CT Ori. Were it not for the low Sc abundances in the atmospheres of DY Aql and CE Vir, the correlations for these two stars would not be significant. Like most of the RV Tauri stars studied in Papers I and II, the depletion diagrams of SS Gem and CT Ori also display a plateau at low condensation temperatures and then a drop beyond about 1000 K. While the data of DY Aql and CE Vir are inconclusive concerning this feature, the drop in abundance does seem to occur at a higher condensation temperature.

The discrepancy between the S and Zn abundances in some of the RV Tauri stars (IW Car, SS Gem, and R Sge) is not explainable by the depletion mechanism, since these two elements have nearly identical condensation temperatures. There are two likely explanations: (1) there is a scatter in initial relative S and Zn abundances, or (2) the differences can be accounted for by errors in the abundance analysis. We believe the second possibility to be the more likely one, especially considering the fact that the discrepancy is much smaller for the weak-lined RV Tauri stars, where line crowding is not a problem.

Combining the results of the present study with those of Papers I and II, we now have photospheric abundance data for nine field RV Tauri stars, all of which show a correlation with $T_{\rm cond}$. The mean abundance pattern (formed from the data of DY Aql, IW Car, SS Gem, CT Ori, DY Ori, AR Pup, R Sge, and CE Vir) shows a fairly tight dependence on $T_{\rm cond}$ (Fig. 4; Table 8). The largest deviations in the trend are due to Si and Mn, which we cannot explain. However, the average scatter in the abundance trend for the RV Tauri stars is no more than that in the interstellar medium (the cool component toward ζ Oph). For instance, the depletion among elements in the interstellar medium with $T_{\rm cond}$ near 1350 K ranges from −1.3 to −2.8 dex (Savage & Sembach 1996); in addition, the amount of depletion of S and Zn differ in the interstellar medium by about 1 dex.

Our detection of lithium in the atmospheres of DY Aql and CE Vir are the first such discoveries in any RV Tauri stars. The strength of the Li I line in the spectra of DY Aql and CE Vir is due primarily to their low effective temperatures; the upper limit of the lithium abundance in our 1994 January 20 spectrum of SS Gem, about 500 K warmer than DY Aql and CE Vir, is only a few tenths of a dex less than the lithium abundance DY Aql and CE Vir. Therefore, it is possible that log ϵ(Li) is near zero in the other RV Tauri stars also.

4.2. *Source of Abundance Patterns*

In Papers I and II we suggested that the selective depletion of elements with high values of $T_{\rm cond}$ in the atmospheres

TABLE 4

INDIVIDUAL ABUNDANCE RESULTS FOR SS GEMINORUM USING THE MODEL ATMOSPHERES IN TABLE 2

Wavelength (Å)	Low E.P. (eV)	log gf	W_λ (mÅ), log ϵ		
			1993 Dec 6	1994 Jan 20	1994 Mar 2, 3
			Li I		
6707.8	0.00	0.17	...	SS, < -0.4	...
			C I		
4770.00	7.48	−2.29	...	...	62, 8.26
4775.88	7.49	−2.15	...	...	72, 8.24
5380.32	7.68	−1.76	95, 8.45	...	...
6587.62	8.53	−0.94	...	...	91, 8.20
7111.45	8.64	−1.32	...	...	63, 8.36
7113.17	8.64	−0.92	...	...	86, 8.24
7116.96	8.65	−1.08	...	...	89, 8.45
			N I		
7442.23	10.23	−0.31	...	...	16, 7.25
7468.40	10.33	−0.13	...	...	54, 7.94
			O I		
6156.80	10.74	−0.45	...	...	19, 8.09
6300.23	0.00	−9.75	...	164, 8.45	...
6363.88	0.02	−10.25	...	...	24, 8.90
			Na I		
6154.23	2.10	−1.57	...	68, 6.22	20, 6.35
6160.75	2.10	−1.27	...	100, 6.23	34, 6.34
			Si I		
5645.62	4.93	−2.14	28, 7.22	52, 7.21	...
5665.56	4.92	−2.04	...	60, 7.20	...
5772.15	5.08	−1.75	...	72, 7.22	...
6125.03	5.61	−1.51	...	35, 7.09	21, 7.51
6145.02	5.61	−1.48	...	46, 7.22	21, 7.48
6721.84	5.56	−1.26	...	63, 7.11	23, 7.27
			S I		
4694.12	6.52	−1.82	...	...	44, 7.16
4695.45	6.52	−1.96	...	...	29, 7.05
4696.26	6.52	−2.19	...	...	21, 7.11
6743.58	7.80	−0.70	...	...	44, 7.15
6748.80	7.86	−0.44	...	...	68, 7.29
6757.16	7.87	−0.29	...	...	76, 7.27
			Ca I		
5512.99	2.93	−0.45	34, 5.30	...	...
5581.98	2.52	−0.55	41, 5.10	...	...
5588.76	2.52	0.36	108, 5.02	...	...
6166.44	2.52	−1.14	...	36, 5.10	...
6169.04	2.52	−0.47	...	72, 4.88	...
6717.69	2.71	−0.52	...	...	29, 5.63
7148.15	2.71	0.14	...	...	104, 6.13
			Sc II		
5239.82	1.45	−0.94	47, 1.25	...	...
5526.82	1.77	−0.22	92, 1.34	...	...
5640.99	1.50	−1.35	33, 1.49	71, 1.59	...
			Ti II		
4544.02	1.24	−2.40	...	...	44, 3.42
4708.67	1.24	−2.37	...	...	62, 3.62
4874.01	3.09	−0.79	46, 3.17	...	...
5185.91	1.89	−1.35	95, 3.05	...	...
5336.79	1.58	−1.63	90, 2.93	...	...

TABLE 4—*Continued*

Wavelength (Å)	Low E.P. (eV)	log *gf*	W_λ (mÅ), log ϵ		
			1993 Dec 6	1994 Jan 20	1994 Mar 2, 3
			Cr I		
4545.96	0.94	−1.37	...	...	43, 5.19
4646.17	1.03	−0.70	...	...	81, 5.12
4651.29	0.98	−1.46	...	...	36, 5.19
4652.17	1.00	−1.03	...	...	57, 5.09
			Cr II		
4884.60	3.86	−2.08	66, 4.66	...	...
5502.09	4.17	−1.99	50, 4.64	...	...
			Mn I		
4709.72	2.89	−0.34	...	...	33, 5.07
4739.11	2.94	−0.49	...	...	25, 5.10
4761.53	2.95	−0.14	...	...	40, 5.04
			Fe I		
4882.15	3.41	−1.49	40, 6.46	...	...
4924.78	2.28	−2.20	101, 6.77	...	...
4930.31	3.96	−1.20	27, 6.48	...	...
4939.69	0.85	−3.33	120, 6.65	...	...
4946.40	3.36	−1.01	90, 6.54	...	...
4969.92	4.21	−0.75	42, 6.53	...	...
4973.10	3.96	−0.85	55, 6.55	...	...
4988.95	4.15	−0.79	59, 6.73	...	...
4994.14	0.91	−3.14	129, 6.62	...	...
5002.80	3.39	−1.44	51, 6.53	...	...
5014.95	3.94	−0.27	92, 6.42	...	...
5022.24	3.98	−0.49	77, 6.48	...	...
5044.22	2.85	−2.04	36, 6.36	...	...
5054.65	3.64	−2.02	13, 6.60	...	...
5074.75	4.22	−0.16	103, 6.73	...	...
5090.78	4.26	0.36	63, 6.47	...	...
5141.75	2.42	−2.16	59, 6.35	...	...
5145.10	2.19	−3.15	20, 6.48	...	...
5364.88	4.45	0.23	105, 6.57	...	...
5373.71	4.47	−0.71	30, 6.53	...	...
5379.58	3.69	−2.11	19, 6.93	...	...
5398.29	4.44	−0.73	31, 6.54	...	...
5417.03	4.41	−1.53	11, 6.78	...	...
5522.45	4.21	−1.40	15, 6.58	...	...
5569.63	3.42	−0.49	115, 6.35	...	...
5572.85	3.40	−0.28	145, 6.54	...	...
5586.77	3.37	−0.12	147, 6.38	...	...
5633.95	4.99	−0.12	28, 6.40	...	...
5638.27	4.22	−0.72	39, 6.43	77, 6.41	...
5679.02	4.65	−0.77	...	40, 6.51	...
5686.53	4.55	−0.45	...	72, 6.47	...
5691.50	4.30	−1.37	...	25, 6.47	...
5731.77	4.26	−1.15	...	57, 6.66	...
5862.37	4.55	−0.39	...	93, 6.61	...
6003.02	3.88	−0.90	...	115, 6.53	...
6056.01	4.73	−0.40	...	66, 6.52	...
6151.62	2.18	−3.29	...	84, 6.54	...
6173.34	2.22	−2.88	...	...	18, 6.99
6191.57	2.43	−1.42	...	...	77, 6.69
6200.31	2.61	−2.44	...	120, 6.54	18, 6.88
6230.73	2.56	−1.28	...	...	105, 7.10
6252.56	2.40	−1.72	...	...	60, 6.72
6335.34	2.20	−2.32	...	...	43, 6.90
6411.66	3.64	−0.66	...	...	62, 6.80
6419.96	4.73	−0.09	...	95, 6.48	41, 6.86
6592.96	2.73	−1.47	...	...	52, 6.65
6593.88	2.43	−2.42	...	...	22, 6.81
6677.99	2.69	−1.44	...	...	68, 6.81
6750.15	2.42	−2.62	...	...	13, 6.75
6806.84	2.73	−3.13	...	49, 6.65	...

TABLE 4—*Continued*

Wavelength (Å)	Low E.P. (eV)	log *gf*	W_λ (mÅ), log ϵ 1993 Dec 6	1994 Jan 20	1994 Mar 2, 3
6810.26	4.61	−0.99	...	34, 6.50	...
7130.92	4.22	−0.70	...	...	39, 7.00
7411.14	4.28	−0.34	...	...	53, 6.92
7445.74	4.26	−0.11	...	...	55, 6.70
			Fe II		
4893.82	2.83	−4.29	60, 6.49	...	...
4993.35	2.80	−3.67	127, 6.66	...	...
5132.67	2.81	−4.00	89, 6.50	...	...
5325.56	3.22	−3.17	130, 6.60	...	...
5414.07	3.22	−3.62	91, 6.54	...	...
5425.26	3.20	−3.21	121, 6.47	...	...
6084.10	3.20	−3.67	...	104, 6.63	65, 6.71
6149.25	3.89	−2.72	...	120, 6.52	101, 6.77
6369.46	2.89	−4.19	...	...	70, 6.88
6416.93	3.89	−2.68	...	114, 6.40	113, 6.93
			Ni I		
4686.22	3.60	−0.64	...	...	19, 5.67
4935.83	3.94	−0.35	23, 5.20	...	...
4937.35	3.61	−0.39	35, 5.15	...	...
5035.37	3.63	0.29	84, 5.12	...	...
5593.75	3.90	−0.84	13, 5.31	...	...
6086.29	4.26	−0.53	...	30, 5.33	...
6111.08	4.09	−0.87	...	32, 5.50	...
6176.81	4.09	−0.53	...	...	14, 5.81
6327.60	1.68	−3.15	...	49, 5.14	...
7122.24	3.54	0.04	...	...	45, 5.41
			Zn I		
4722.16	4.03	−0.39	...	...	105, 4.93
6362.54	5.79	0.27	...	...	35, 4.67
			Y II		
5087.43	1.08	−0.17	108, 0.64	...	...
5402.78	1.84	−0.57	39, 0.98	...	...
			Eu II		
6437.64	1.32	−0.27	...	...	12, 0.19
6645.13	1.38	0.20	...	...	19, 0.00

of RV Tauri stars is due to the formation of grains, which are pushed away from the star by radiation pressure without dragging significant amounts of gas with them. Hence, the original metallicity of a depleted RV Tauri star should be given not by the abundance of Fe, the traditional indicator of metallicity, but by the present abundances of S and Zn (C, N, O, or Na are likely unreliable indicators of the original metallicity because the abundances of these elements might be affected by dredge-ups). One way to represent the amount of depletion is by comparing the S and Zn abundances to the Fe abundances (Fig. 5). On the assumption that the extraordinarily high S/Fe and Zn/Fe ratios result from depletion of Fe, Figure 5 implies that the original metallicities were in the range $-1 < [\mathrm{Fe/H}] < 0$. Also shown in Figure 5 are two metal-depleted post-AGB stars with values of [Fe/H] similar to the RV Tauri stars.

What is new in the present study is the finding that the depletion pattern is still present even in the atmospheres of stars with $T_{\mathrm{eff}} \simeq 4250$ K; to date DY Aql and CE Vir are the coolest stars displaying a correlation with T_{cond}. If, as suggested in Paper II, the atmosphere of an RV Tauri star is depleted by the selective loss of grains, then the entire convective envelope must be depleted if the depletion pattern is to be maintained. It is not surprising to find depletion patterns among the F supergiants, which have relatively small outer convective regions. The convective regions of DY Aql and CE Vir are no doubt much larger, and, not surprisingly, we see a less pronounced depletion pattern in these stars.

What is not clear is whether the observed pattern in these stars is maintained by ongoing depletion or whether it is a residual feature of past activity. A possible discriminant might be the presence of infrared emission from these stars. Warm emission would support the view that the depletion is ongoing and cool emission that it has ceased. Comparing the RV Tauri stars' $\langle m_v \rangle_0 - 3.6\ \mu$m color to that of the supergiant α Per (using data tabulated by Gezari et al. 1993), we find that all but SS Gem show some excess infrared emission. The infrared excess does not correlate with the degree of depletion (as given by [S/Fe]). IW Car and AR Pup have the largest infrared excess at 3.6 μm; they also have strong emission at 25 μm as measured by the *IRAS* satellite. This implies that dust emission has been ongoing

TABLE 5

INDIVIDUAL ABUNDANCE RESULTS FOR CT ORIONIS USING THE MODEL ATMOSPHERES IN TABLE 2

WAVELENGTH (Å)	LOW E.P. (eV)	log *gf*	W_λ (mÅ), log ϵ	
			1995 Dec 10, 11	1996 Apr 9, 10
		Li I		
6707.8	0.00	0.17	SS, <1.0	...
		C I		
4932.07	7.68	−1.77	...	59, 8.01
5380.32	7.68	−1.76	...	56, 7.98
6587.62	8.53	−0.94	31, 7.94	38, 7.69
7113.17	8.64	−0.92	35, 8.12	...
7116.96	8.65	−1.08	39, 8.37	...
		O I		
6300.23	0.00	−9.75	40, 8.22	...
6363.88	0.02	−10.25	20, 8.36	...
		Na I		
5688.22	2.10	−0.40	117, 6.43	98, 6.02
8183.25	2.10	0.22	204, 6.95	...
		Mg I		
5528.42	4.34	−0.34	...	78, 5.76
5711.08	4.34	−1.68	27, 6.23	...
		Si I		
6721.84	5.56	−1.26	22, 6.85	...
		S I		
6052.68	7.87	−0.63	...	22, 6.66
6748.80	7.86	−0.44	41, 7.13	36, 6.76
6757.16	7.87	−0.29	41, 6.99	47, 6.80
		Ca I		
5588.76	2.52	0.36	...	39, 4.35
6122.23	1.89	−0.31	...	51, 4.59
6439.08	2.52	0.39	75, 4.75	50, 4.47
7148.15	2.71	0.14	47, 4.70	...
		Sc II		
5031.01	1.36	−0.26	43, 0.76	31, 0.67
5239.82	1.45	−0.94	30, 1.11	...
		Ti II		
4805.10	2.06	−1.10	...	51, 2.87
5336.79	1.58	−1.63	24, 2.35	33, 2.78
5381.03	1.57	−1.97	30, 2.81	...
		Cr I		
5206.04	0.94	0.02	...	102, 4.07
5208.43	0.94	0.16	...	113, 4.12
		Cr II		
4824.14	3.87	−1.22	...	81, 4.30
5237.32	4.07	−1.16	39, 3.91	29, 3.63
5313.59	4.07	−2.10	...	17, 4.29
		Fe I		
4871.32	2.85	−0.36	...	83, 5.65
4872.14	2.88	−0.57	...	64, 5.64
4890.76	2.87	−0.39	...	81, 5.67
4891.50	2.85	−0.11	...	106, 5.69
4919.00	2.85	−0.34	...	78, 5.57
4920.51	2.83	0.07	...	111, 5.57
5001.87	3.88	0.01	...	30, 5.46

TABLE 5—*Continued*

WAVELENGTH (Å)	LOW E.P. (eV)	log *gf*	W_λ (mÅ), log ϵ	
			1995 Dec 10, 11	1996 Apr 9, 10
5049.83	2.28	−1.35	62, 5.58	...
5068.77	2.94	−1.04	36, 5.49	...
5133.69	4.18	0.20	47, 5.71	47, 5.83
5162.27	4.18	0.08	41, 5.72	...
5191.47	3.04	−0.55	59, 5.50	...
5192.35	3.00	−0.42	67, 5.48	...
5215.19	3.26	−0.87	41, 5.73	...
5216.27	1.61	−2.12	55, 5.51	...
5232.94	2.94	−0.08	95, 5.64	100, 5.61
5302.31	3.28	−0.74	...	42, 5.84
5324.18	3.21	−0.10	88, 5.78	74, 5.57
5339.93	3.27	−0.68	...	42, 5.77
5367.48	4.42	0.44	37, 5.52	38, 5.65
5369.97	4.37	0.54	...	61, 5.85
5383.38	4.31	0.65	54, 5.51	55, 5.60
5393.17	3.24	−0.72	49, 5.69	...
5397.14	0.91	−1.99	107, 5.63	96, 5.51
5405.78	0.99	−1.85	115, 5.79	...
5415.21	4.39	0.64	54, 5.60	45, 5.54
5434.53	1.01	−2.12	87, 5.45	74, 5.51
5446.92	0.99	−1.91	...	115, 5.79
5497.52	1.01	−2.84	...	35, 5.67
5586.76	3.37	−0.12	71, 5.60	62, 5.60
5615.66	3.33	0.05	...	90, 5.74
7495.08	4.22	0.36	60, 5.69	...
		Fe II		
5197.58	3.23	−2.25	98, 5.99	95, 5.64
5325.56	3.22	−3.17	...	32, 5.65
5425.26	3.20	−3.21	27, 5.58	30, 5.62
6416.93	3.89	−2.68	11, 5.23	...
6432.28	2.89	−3.58	33, 5.70	...
		Ni I		
4904.42	3.54	−0.17	...	17, 4.67
5476.92	1.83	−0.89	...	79, 4.79
6767.78	1.83	−2.17	22, 4.76	...
		Zn I		
4810.54	4.08	−0.17	...	92, 4.04
6362.54	5.79	0.27	23, 3.94	...
		Y II		
4883.69	1.08	−0.04	...	33, 0.08
		Ba II		
5853.69	0.60	−1.00	...	61, 0.55

for these two RV Tauri stars.

Our Li abundance estimates for DY Aql and CE Vir are not exceptional. These stars cannot be considered Li-rich in the traditional sense of the phrase; Luck & Lambert (1982) find that the mean value of log ϵ(Li) in a sample of 25 M giants is about -0.2, the same as our mean estimate for DY Aql and CE Vir. Hence, the present abundance of lithium in these two RV Tauri stars probably resulted from the same processes that operate in the normal field M giants. While lithium is depleted by about 1.5 dex in the interstellar medium (Savage & Sembach), our estimates should not require a large depletion correction, since Sc is the only element that appears to be obviously depleted in DY Aql and CE Vir. Clearly, the presence of Li does not require its production on the AGB (or at an earlier stage). This is likely consistent with current theoretical ideas about Li production by hot bottom convection (HBC) occurring only in the more massive AGB stars. The possibility remains that Li was produced and destroyed by the AGB progenitor—destruction necessarily occurs if HBC is sufficiently prolonged. The relatively large distances above the Galactic plane of DY Aql and CE Vir favor their being low-mass stars, which are predicted to be incapable of Li production by HBC.

Often, *s*-process element enhancement is taken as evidence of dredge-up. A clear indication of enhancement becomes more difficult when another process affecting the surface abundances, e.g. depletion of high $T_{\rm cond}$ elements, is in operation. Even so, given the amount of depletion of Y in the RV Tauri stars relative to other elements with similar values of $T_{\rm cond}$, it appears that the abundances of the *s*-process elements are not significantly enhanced in these

TABLE 6

INDIVIDUAL ABUNDANCE RESULTS FOR CE VIRGINIS USING THE MODEL ATMOSPHERES IN TABLE 2

WAVELENGTH (Å)	LOW E.P. (eV)	log *gf*	W_λ (mÅ), log ϵ			
			1994 Jan 20	1995 Jan 24	1996 Apr 9	1996 Jul 19
			Li I			
6707.8	0.00	0.17	SS, −0.40	...	SS, −0.17	SS, −0.03
			Na I			
5682.65	2.10	−0.71	82, 5.12	...	69, 5.08	83, 5.18
5688.22	2.10	−0.40	121, 5.23	...	...	...
6154.23	2.10	−1.57	21, 5.09	...	...	...
			Mg I			
5711.10	4.34	−1.68	168, 7.06	...	167, 6.98	161, 7.08
			Si I			
5772.15	5.08	−1.75	74, 7.03	65, 6.95	63, 6.92	...
6125.03	5.61	−1.51	36, 6.92	...	28, 6.82	33, 6.86
6145.02	5.61	−1.48	47, 7.06	35, 6.92	...	...
			Si II			
6347.09	8.12	0.26	37, 7.25	...	52, 7.35	...
6371.34	8.12	−0.05	...	...	38, 7.38	...
			Ca I			
5581.98	2.52	−0.56	...	...	97, 4.87	...
5601.29	2.52	−0.52	...	...	102, 4.87	...
6166.44	2.52	−1.14	55, 4.79	...	...	60, 4.89
6717.69	2.71	−0.52	95, 4.80	100, 5.00	...	...
			Sc II			
5526.79	1.77	−0.22	...	...	42, 0.69	...
6604.60	1.36	−1.53	24, 0.98	...	18, 1.08	14, 0.65
			Ti I			
5866.45	1.07	−0.78	...	149, 4.01	...	...
5965.83	1.88	−0.35	70, 3.67	...	81, 4.10	...
			Mn I			
4739.11	2.94	−0.49	...	...	...	50, 3.67
6013.48	3.07	−0.25	67, 3.57	57, 3.70	61, 3.75	75, 3.66
6021.79	3.08	0.03	108, 3.74	97, 3.80	95, 3.80	105, 3.76
			Fe I			
5560.21	4.43	−1.04	...	...	54, 6.38	...
5633.95	4.99	−0.12	...	...	64, 6.26	...
5679.02	4.65	−0.77	59, 6.32	...	52, 6.35	...
5705.47	4.30	−1.36	...	...	36, 6.30	...
5717.83	4.28	−0.98	81, 6.29	...	76, 6.35	81, 6.33
5809.22	3.88	−1.69	...	...	59, 6.38	...
5814.81	4.28	−1.82	...	...	16, 6.32	...
5852.22	4.55	−1.18	...	37, 6.42	38, 6.44	40, 6.34
5859.80	4.55	−0.67	...	...	77, 6.38	...
5862.37	4.55	−0.39	103, 6.31	104, 6.35	101, 6.33	96, 6.27
6027.05	4.08	−1.09	82, 6.10	79, 6.20	...	86, 6.18
6056.01	4.73	−0.40	80, 6.26	79, 6.32	68, 6.23	74, 6.22
6079.01	4.65	−0.97	55, 6.43	48, 6.46	34, 6.28	...
6093.64	4.61	−1.35	30, 6.39	...	17, 6.27	...
6096.66	3.98	−1.78	...	...	37, 6.30	...
6165.36	4.14	−1.47	44, 6.10	42, 6.25	...	47, 6.15
6180.21	2.73	−2.65	...	...	...	125, 6.31
6200.31	2.61	−2.44	152, 6.17	158, 6.36	...	...
6226.74	3.88	−2.22	...	...	...	37, 6.41
6322.69	2.59	−2.43	...	171, 6.43	164, 6.37	166, 6.36
6380.74	4.19	−1.32	...	...	60, 6.36	70, 6.34
6419.96	4.73	−0.09	...	113, 6.31	94, 6.15	...
6609.11	2.56	−2.69	...	...	129, 6.24	...
6703.55	2.76	−3.05	80, 6.16	77, 6.41	70, 6.36	88, 6.27
6710.32	1.48	−4.88	...	...	...	91, 6.31

TABLE 6—*Continued*

Wavelength (Å)	Low E.P. (eV)	log gf	W_λ (mÅ), log ϵ 1994 Jan 20	1995 Jan 24	1996 Apr 9	1996 Jul 19
6726.67	4.61	−1.00	...	...	...	43, 6.20
6739.52	1.56	−4.95	...	...	...	74, 6.32
6750.15	2.42	−2.62	184, 6.32	180, 6.42	166, 6.28	179, 6.34
6752.71	4.64	−1.20	...	...	30, 6.39	39, 6.38
6806.84	2.73	−3.13	...	76, 6.43	...	...
6820.37	4.64	−1.17	...	30, 6.35	...	34, 6.27
7130.92	4.22	−0.70	...	120, 6.28	...	...
7445.74	4.26	−0.11	...	...	...	165, 6.21
7511.03	4.18	0.10	...	...	...	205, 6.36
			Fe II			
5425.26	3.20	−3.21	...	...	...	79, 6.30
5991.37	3.15	−3.56	...	...	58, 6.28	...
6084.10	3.20	−3.67	59, 6.56	...	51, 6.50	...
6247.55	3.89	−2.34	...	...	...	88, 6.36
6369.46	2.89	−4.19	...	49, 6.53	47, 6.45	45, 6.24
6416.93	3.89	−2.68	48, 6.12	...	...	...
6432.28	2.89	−3.58	68, 6.05	76, 6.23	66, 6.06	...
			Co I			
5647.23	2.28	−1.56	54, 3.75	...	37, 3.84	53, 3.75
6116.99	1.79	−2.49	...	30, 3.97	...	...
			Ni I			
6111.08	4.09	−0.87	28, 4.96	31, 5.18	23, 5.03	31, 5.03
6767.77	1.83	−2.17	...	207, 5.21	...	...
			Zn I			
4722.16	4.03	−0.39	...	...	...	114, 3.92
6362.54	5.79	0.27	...	...	31, 3.82	...
			Ba II			
5853.68	0.60	−1.00	162, 0.52	169, 0.66	...	152, 0.43
			Eu II			
6645.13	1.38	0.20	36, −0.67	32, −0.46	28, −0.58	38, −0.71

stars. This may indicate the stars left the AGB before He-shell flashes led to *s*-process enrichment of the envelopes.

While the mean abundance pattern in the atmospheres of RV Tauri stars is similar to that in the interstellar medium, there are some significant differences. For instance, the gas-phase abundances in the interstellar medium drop off more steeply (especially beyond $T_{\rm cond} = 1300$ K) than in the RV Tauri stars. Also, Ca is more depleted in the interstellar medium than Ti, while the reverse is true in the RV Tauri stars. Gonzalez & Wallerstein (1996) observed the same pattern in ST Pup, a type II Cepheid; they suggested that excess ionization, produced by a shock, prevented Ca from sticking to grains in the tenuous outer layers of the star. The relative Ca and Ti abundances also depend on the total H gas density along the line of sight (Jenkins 1987); at a low gas density, the relative amounts of depletion of Ca and Ti are similar, but Ca becomes more strongly depleted at higher densities.

Using basic stellar equations relating luminosity, mass, $T_{\rm eff}$, and g and adopting Boothroyd & Sackmann's (1988, eq. [15], applicable to stars with core masses between 0.5 and 0.7 $M_\odot$) core mass-luminosity relation, we find that for AGB stars the surface gravity relates to $T_{\rm eff}$ in the following way: $\log g = {\rm const.} + 4 \log T_{\rm eff}$. If the RV Tauri stars in our sample all have roughly the same present mass, then on a plot of $\log g$ versus $\log T_{\rm eff}$, the slope of a line drawn through the data points should be close to 4.0. This is not what we find (Fig. 6). The individual estimates for SS Gem and R Sge do fall along a single line with a slope close to 4.0 (Fig. 6, *dashed line*). However, the other RV Tauri stars fall on a distinctly different part of the $\log g$-$\log T_{\rm eff}$ plot; they have a higher surface gravity at a given temperature (they fall near the dotted line in Fig. 6; we cannot account for the distribution of points for CE Vir). If these two groups of RV Tauri stars have very different core masses, then one cannot apply a single core mass-luminosity relation or a single $\log g$-$\log T_{\rm eff}$ relation. Also included in Figure 6 are the data for the M5 giants, which have masses near 0.6 $M_\odot$; they fall closer to dotted line in the figure. These two groups differ in other ways as well; on average, SS Gem and R Sge have smaller distances above the Galactic plane than the other group; the initial abundances of SS Gem and R Sge, as given by the S and Zn abundances, are roughly solar, while for EP Lyr, CT Ori, and CE Vir, they are less than solar. These differences point toward SS Gem and R Sge being members of the thin disk and hence of moderate mass, while the other RV Tauri stars are less massive members of the thick disk.

TABLE 7

Final Adopted Abundances for DY Aquilae, SS Geminorum, CT Orionis, and CE Virginis

Species; log $\epsilon_\odot$	DY Aql		SS Gem		CT Ori		CE Vir	
	[X/Fe]	[X/H]	[X/Fe]	[X/H]	[X/Fe]	[X/H]	[X/Fe]	[X/H]
(1)	(2)	(3)	(4)	(5)	(6)	(7)	(8)	(9)
Li I; 3.31	-2.23 ± 0.10	-3.26 ± 0.10	< -2.8	< -3.7	< -0.4	< -2.3	-2.30 ± 0.10	-3.49 ± 0.10
C I; 8.71..........	...	...	0.31 ± 0.07	-0.56 ± 0.23	1.18 ± 0.08	-0.69 ± 0.19	...	...
N I; 7.97	...	...	0.29 ± 0.25	-0.58 ± 0.33	...	...	...	...
O I; 8.97	...	...	0.28 ± 0.21	-0.59 ± 0.30	1.19 ± 0.05	-0.68 ± 0.22	...	...
Na I; 6.28	0.20 ± 0.18	-0.83 ± 0.31	0.83 ± 0.05	-0.04 ± 0.16	2.06 ± 0.22	0.19 ± 0.22	0.08 ± 0.03	-1.11 ± 0.15
Mg I; 7.67	...	...	...	...	0.20 ± 0.18	-1.67 ± 0.18	0.58 ± 0.04	-0.61 ± 0.15
Si I, II; 7.40	0.52 ± 0.18	-0.51 ± 0.26	0.74 ± 0.03	-0.13 ± 0.13	1.32 ± 0.12	-0.55 ± 0.12	0.81 ± 0.06	-0.38 ± 0.17
S I; 7.38	...	...	0.45 ± 0.03	-0.42 ± 0.22	1.34 ± 0.07	-0.53 ± 0.16	...	...
Ca I; 6.37	-0.19 ± 0.06	-1.22 ± 0.24	-0.18 ± 0.11	-1.05 ± 0.15	0.07 ± 0.07	-1.80 ± 0.08	-0.30 ± 0.02	-1.49 ± 0.18
Sc II; 3.43	-1.10 ± 0.18	-2.13 ± 0.22	-1.05 ± 0.07	-1.92 ± 0.11	-0.71 ± 0.11	-2.58 ± 0.12	-1.38 ± 0.11	-2.57 ± 0.23
Ti I, II; 5.21	...	...	-1.13 ± 0.06	-2.00 ± 0.11	-0.64 ± 0.10	-2.51 ± 0.12	-0.10 ± 0.11	-1.29 ± 0.22
Cr I, II; 5.76......	...	...	-0.02 ± 0.04	-0.89 ± 0.15	0.16 ± 0.09	-1.71 ± 0.13	...	...
Mn I; 5.64	-0.52 ± 0.18	-1.55 ± 0.19	0.09 ± 0.01	-0.78 ± 0.15	...	...	-0.73 ± 0.02	-1.92 ± 0.05
Fe I, II; 7.50......	-1.03 ± 0.09		-0.87 ± 0.11		-1.87 ± 0.07		-1.19 ± 0.07	
Co I; 4.89	0.31 ± 0.18	-0.72 ± 0.19	...	...	...	...	0.13 ± 0.04	-1.06 ± 0.06
Ni I; 6.23.........	-0.03 ± 0.18	-1.06 ± 0.19	0.02 ± 0.04	-0.85 ± 0.12	0.38 ± 0.05	-1.49 ± 0.08	0.03 ± 0.03	-1.16 ± 0.06
Zn I; 4.57	...	...	0.89 ± 0.09	0.02 ± 0.17	1.29 ± 0.04	-0.58 ± 0.05	0.49 ± 0.06	-0.70 ± 0.07
Y II; 2.26	...	...	-0.49 ± 0.12	-1.36 ± 0.14	-0.31 ± 0.12	-2.18 ± 0.15	...	...
Ba II; 2.39........	...	...	...	...	0.03 ± 0.12	-1.84 ± 0.15	-0.66 ± 0.05	-1.85 ± 0.20
Eu II; 0.60	0.04 ± 0.18	-0.99 ± 0.23	...	...	...	...	-0.02 ± 0.05	-1.21 ± 0.20

Note.—The abundances are averages of the results listed in Tables 3, 4, 5, and 6. The standard deviations of the means listed in cols. (2), (4), (6), and (8) were estimated from the line-to-line scatter; those listed in cols. (3), (5), (7), and (9) were estimated using the results of Table 4 of Paper II. For a value of [X/Fe] based on a single abundance estimate, such as Ba II, the standard deviation of the Fe I lines of the spectrum containing the line is quoted instead. The solar abundance of Li listed in col. (2) is the meteoritic value quoted by Anders & Grevesse 1989.

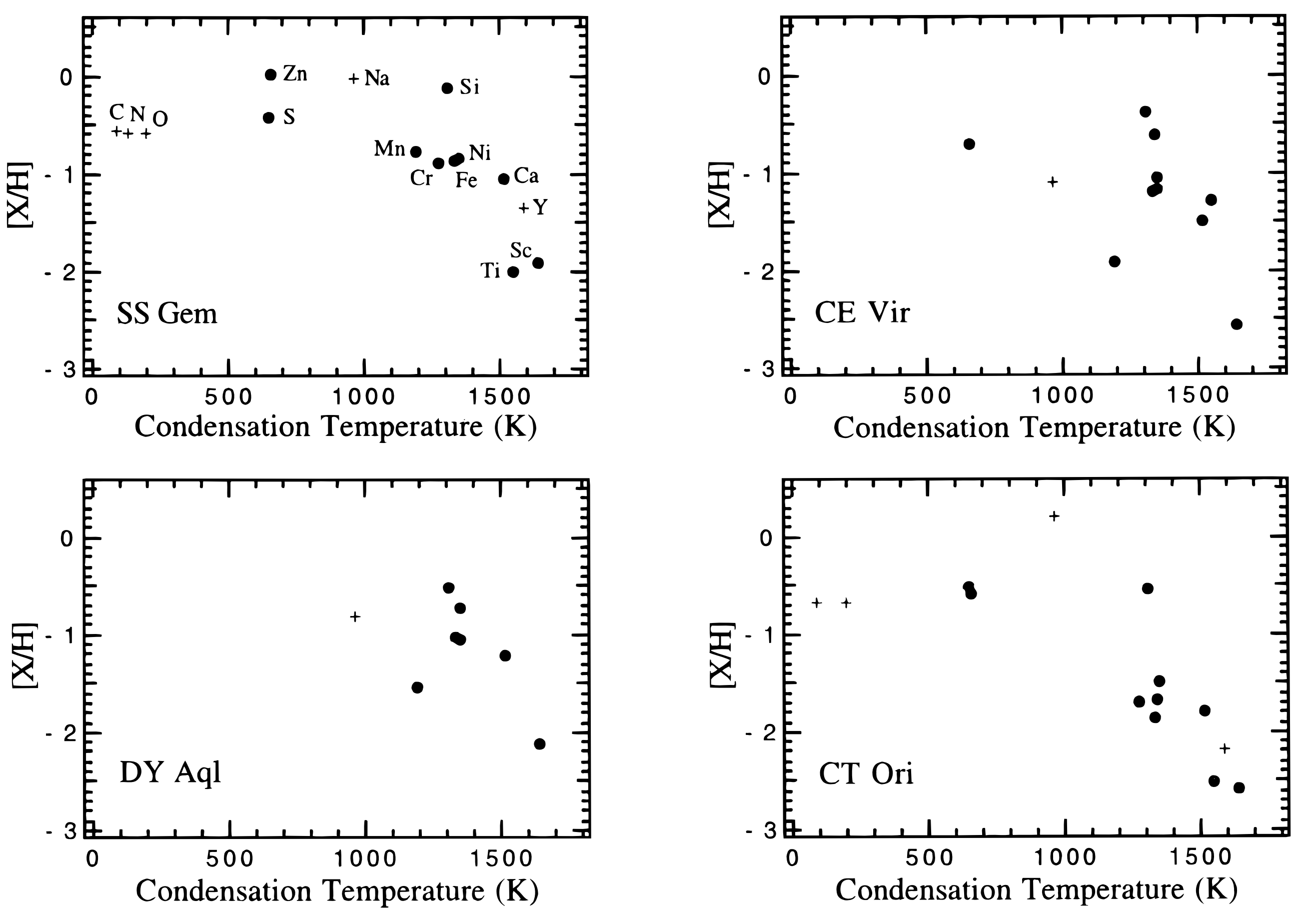

Fig. 3.—Abundances, as [X/H], of the four RV Tauri stars in this study vs. condensation temperature. The plus signs represent those elements whose abundances might be affected by dredge-up (C, N, O, Na, Y). The condensation temperatures have been calculated by Wasson (1985) assuming a solar mix and a pressure of 10^{-1} atm.

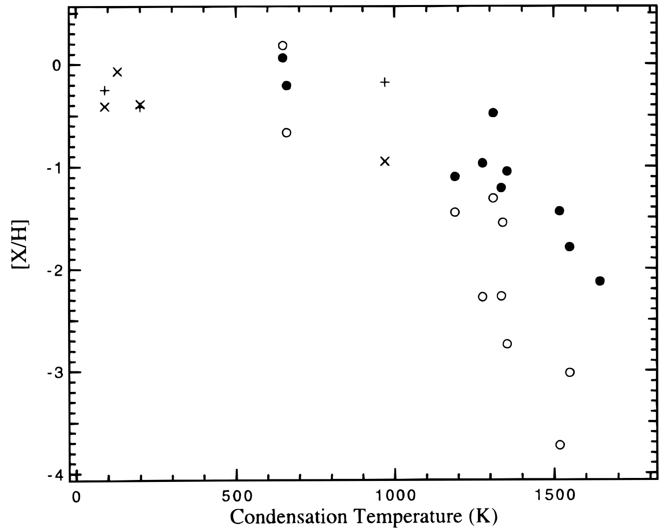

FIG. 4.—Mean abundances vs. condensation temperature for field RV Tauri stars (*filled circles and plus signs*): DY Aql, IW Car, SS Gem, CT Ori, DY Ori, AR Pup, R Sge, CE Vir. EP Lyr was not included because it has a different abundance pattern compared to the other field RV Tauri stars. Also shown are the interstellar abundances along the line of sight to ζ Ophiuchi (Savage & Sembach 1996; *open circles and crosses*).

SS Gem and R Sge share another similarity—they have relatively small values of [S/Fe]; CE Vir, which is cooler on average, has a similarly small value of [Zn/Fe]. This implies that the amount of depletion depends on surface gravity and temperature.

4.3. *A Depletion Index*

As shown in the present study, Papers I and II, and Gonzalez & Wallerstein (1996), Sc and Ti have the lowest abundances in depleted pulsating luminous stars. Hence, we can form indices, such as [Sc/Fe] and [Ti/Fe], as a measure of the degree of depletion in these stars. Unfortunately, accurate estimates of [Sc/Fe] and [Ti/Fe] for a given star require detailed abundance analyses of the type presented here. In order to test the possibility of estimating [Sc/Fe] from W_λ estimates of Sc and Fe lines alone, we have measured the W_λ-values of the Sc II line at 5526 Å and the Fe II line at 5425 Å in the spectra of seven stars (Table 9). These two lines were selected for several reasons: they have similar wavelengths, they are similar in strength in luminous stars, and they are of the same ionization state. The quantity [Sc/Fe] has been parameterized in the following way:

$$[\mathrm{Sc/Fe}] = C_0 + C_1 \log (W_\lambda/\lambda)_{\mathrm{Fe}} - C_2[\log (W_\lambda/\lambda)_{\mathrm{Sc}} - \log (W_\lambda/\lambda)_{\mathrm{Fe}}] , \quad (1)$$

where the derived values of the coefficients from a least-squares fit are $C_0 = 0.43 \pm 1.19$, $C_1 = 0.23 \pm 0.24$, $C_2 = 1.51 \pm 0.29$. Also shown in Table 9 are the values of [Sc/Fe] calculated using equation (1); the predicted values are within about 0.2 dex of the measured values, except for α Per, where the predicted value is too small by about 0.4 dex. As a predictor, then, equation (1) can distinguish depleted stars from nondepleted ones if $[\mathrm{Sc/Fe}]_{\mathrm{pred}} < -0.5$. Treating EP Lyr as an unknown, we would not be able to conclude

TABLE 8

MEAN ABUNDANCES OF FIELD RV TAURI STARS

Element	[X/H]	T_{cond}
C	−0.25 ± 0.38	90
O	−0.42 ± 0.34	200
Na	−0.18 ± 0.51	970
Si	−0.48 ± 0.44	1311
S	0.06 ± 0.43	648
Ca	−1.44 ± 0.36	1518
Sc	−2.13 ± 0.39	1644
Ti	−1.79 ± 0.58	1549
Cr	−0.97 ± 0.59	1277
Mn	−1.10 ± 0.79	1190
Fe	−1.21 ± 0.59	1336
Ni	−1.05 ± 0.32	1354
Zn	−0.21 ± 0.36	660

NOTE.—The standard deviation given for each abundance estimate was calculated from the scatter in the abundances estimates.

TABLE 9

[Sc/Fe] ESTIMATES FROM THE 5526 Å Sc II AND 5425 Å Fe II LINES

Spectrum	$-\log (W_\lambda/\lambda)_{\mathrm{Sc}}$	$-\log (W_\lambda/\lambda)_{\mathrm{Fe}}$	$[\mathrm{Sc/Fe}]_{\mathrm{meas}}$	$[\mathrm{Sc/Fe}]_{\mathrm{pred}}$
Calibrators				
CT Ori, 1996 Apr 10	5.36	5.22	−0.71	−0.98
SS Gem, 1993 Dec 6	4.79	4.61	−1.05	−0.90
EP Lyr, 1994 Jun 27	5.09	5.37	−0.31	−0.38
EP Lyr, 1995 Jun 12	4.87	5.20	−0.31	−0.28
EP Lyr, 1996 Mar 3	4.77	5.22	−0.31	−0.09
R Sge, 1995 Jun 12 10	4.44	4.28	−0.98	−0.80
α Per	4.29	4.40	−0.02	−0.42
CE Vir, 1994 Feb 5	5.33	4.82	−1.38	−1.45
CE Vir, 1996 Jul 19	5.17	4.85	−1.38	−1.17
ST Pup, 1994 Feb 5	4.92	4.96	−0.72	−0.65
Unknowns				
TW Cam, 1994 Aug 25	4.49	4.55		−0.53
AC Her, 1996 Apr 10	5.60	5.06		−1.55
TT Oph, 1996 Apr 10	4.49	4.63		−0.42
V453 Oph, 1994 Aug 18	4.93	5.48		0.00
V564 Oph, 1994 Aug 18	4.65	5.12		−0.04
SV UMa, 1996 Apr 10	4.54	4.84		−0.23
RX Vir, 1995 Jun 12	4.74	4.96		−0.38

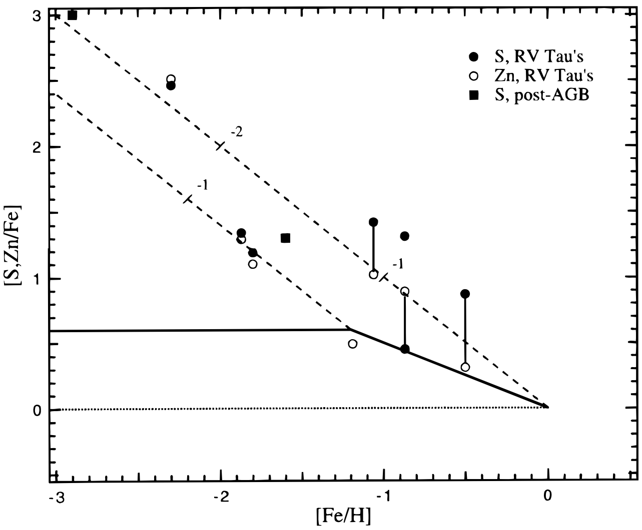

FIG. 5.—Sulfur and zinc abundances of field RV Tauri and post-AGB stars (HD 46703 and BD +39 4926; data from Waelkens et al. 1992). The solid line is the mean trend of S abundances among field dwarfs, and the dotted line is trend for Zn (Lambert 1989). The dashed lines show the change in [S,Zn/Fe] as [Fe/H] is reduced for two starting points on the solid line. Also shown are tick marks indicating the amount of depletion of Fe in dex. This diagram is consistent with the hypothesis that the initial metallicities of the field RV Tauri stars were between 0 and −1.

that it is a depleted star using equation (1), but the other depleted stars in Table 9 would be recognized as such. Also included in Table 9 are several "unknowns," all luminous variables. Of these, AC Her and TW Cam are the most likely to be depleted.

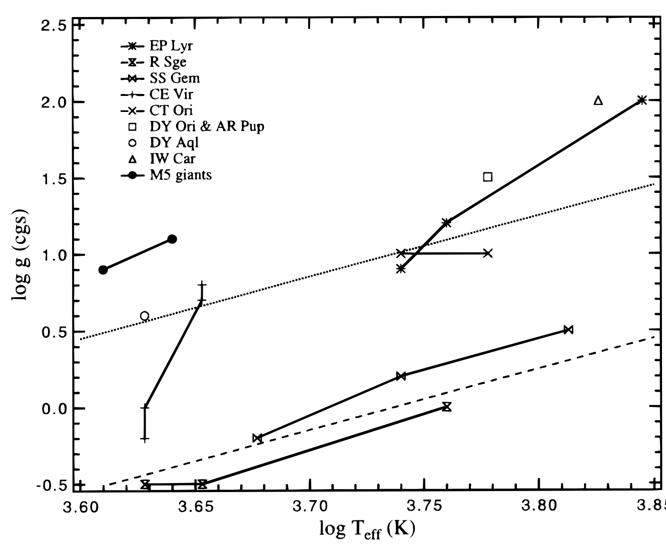

FIG. 6.—Spectroscopic estimates of log g and log $T_{\rm eff}$ for each spectrum of all nine field RV Tauri stars are shown. The solid lines connect estimates for a given star, except for the M5 giants, where the line represents several stars (data from Sneden et al. 1992). The dotted and dashed lines each have a slope of 4.0.

5. CONCLUSIONS

The results of our spectroscopic abundance analyses of DY Aql, SS Gem, CT Ori, and CE Vir continue to verify the trends reported in Papers I and II—the abundances correlate with $T_{\rm cond}$. Surprisingly, the correlation continues to exist even among some of the coolest RV Tauri stars. Some elements deviate from the abundance-$T_{\rm cond}$ trend among some of our targets; specifically, Mn is too low and Si is too high. The scatter in the mean abundance-$T_{\rm cond}$ relation (formed from the abundance results of eight RV Tauri stars) is similar to that determined for the interstellar medium.

The presence of a strong Li I resonance line in two of our sample stars is due to their low temperatures; their lithium abundances are not exceptional. More importantly, we have found some evidence that there are two distinct groups of stars (based on spectroscopic parameters and location in the Galaxy) among the sample of field RV Tauri stars: one group probably belonging to the thin disk (SS Gem and R Sge), the other to the thick disk (DY Aql, IW Car, EP Lyr, CT Ori, DY Ori, AR Pup, and possibly CE Vir). There are probably no halo stars in our current sample of field RV Tauri stars.

In this series of papers, we have shown that the atmospheres of the RV Tauri stars have experienced depletion of the elements that are easily condensed onto grains. This phenomenon of depletion has previously been seen in the post-AGB stars (spectral types A–G; Van Winckel, Mathis, & Waelkens 1992) and in young main-sequence stars known as the λ Boo stars (Venn & Lambert 1990; Sturenburg 1993). Van Winckel, Waelkens, & Waters (1995) have shown that all the most extreme of the depleted post-AGB stars are binaries. This link to binarity encourages the speculation that the dust-gas separation occurs in a circumbinary disk (Waters, Trams, & Waelkens 1992) and would occur, if at all, only mildly for single post-AGB stars. The occurrence of severe depletion in all RV Tauri stars implies either that all RV Tauri stars are as yet unrecognized spectroscopic binaries or that the depletion may occur efficiently in the upper photosphere or inner circumstellar shell of single stars. In Paper II, we suggested that the winds required to account for the observed infrared excess might well achieve severe depletion in single stars. It will be a challenge to prove that RV Tauri stars are spectroscopic binaries as the orbital radial velocity variations are most likely smaller than the pulsational variation of radial velocity. This is an important observational test to make, because if it is shown that all RV Tauri stars are spectroscopic binaries, then it will be clear that these stars, like Barium stars, owe their origin to binarity.

We thank J. Tomkin for obtaining a spectrum of CE Vir at our request. We also thank R. E. Luck for providing us with his compilation of laboratory *gf*-value, R. L. Kurucz for the use of his model stellar atmospheres, and C. Sneden for the use of his LTE abundance analysis code, MOOG. This research has been supported in part by the National Science Foundation (grant no. AST 93-15124) and the Robert A. Welch Foundation of Houston, Texas.

REFERENCES

Anders, G., & Grevesse, W. 1989, Geochim. Cosmochim. Acta, 53, 197
Anderson, J., Gustafsson, B., & Lambert, D. L. 1984, A&A, 136, 165
Boothroyd, A. I., & Sackmann, I.-J. 1988, ApJ, 328, 641
Burnstein, D., & Heiles, C. 1982, AJ, 87, 1165
Cunha, K., Smith, V. V., & Lambert, D. L. 1995, ApJ, 452, 634
Dawson, D. W. 1979, ApJS, 41, 97
Dawson, D. W., & Patterson, C. R. 1982, PASP, 94, 574
Dupuy, D. L. 1973, ApJ, 185, 597

Gezari, D. Y., Schmitz, M., Pitts, P. S., & Mead, J. M. 1993, Catalog of Infrared Observations (NASA Ref. Pub. 1294)
Giridhar, S., Rao, N. K., & Lambert, D. L. 1994, ApJ, 437, 476 (Paper I)
Goldsmith, M. J., Evans, A., Albinson, J. S., & Bode, M. F. 1987, MNRAS, 227, 143
Gonzalez, G. 1994, AJ, 108, 1312
Gonzalez, G., & Lambert, D. L. 1996, AJ, 111, 424
Gonzalez, G., Lambert, D. L., & Giridhar, S. 1996, ApJ, in press (Paper II)
Gonzalez, G., & Wallerstein, G. 1994, AJ, 108, 1325
———. 1996, MNRAS, 280, 515
Jenkins, E. B. 1987, in Interstellar Processes, ed. D. J. Hollenbach & H. A. Thronson, Jr. (Dordrecht: Reidel), 533
Kurucz, R. 1993, ATLAS9 Stellar Atmosphere Programs and 2km/s Grid CD-ROM vol. 13 (Cambridge: Smithsonian Astrophys. Obs.)
Kurucz, R. L., Furenlid, I., Brault, J., & Testerman, L. 1984, Solar Flux Atlas from 296 to 1300 nm (Sunspot: NSO)
Lambert, D. L. 1989, Cosmic Abundances of Matter, ed. C. J. Waddington (New York: AIP), 168
Lambert, D. L., Heath, J. E., Lemke, M., & Drake, J. 1996, ApJS, 103, 183
Luck, R. E., & Lambert, D. L. 1982, ApJ, 256, 189
McCarthy, J. K., Sandiford, B. A., Boyd, D., & Booth, J. 1993, PASP, 105, 881
Nave, G., Johansson, S., Learner, R. C. M., Thorne, A. P., & Brault, J. W. 1994, ApJS, 94, 221
Neckel, Th., & Klare, G. 1980, A&AS, 42, 251
Preston, G. W., Krzeminski, W., Smak, J., & Williams, J. A. 1963, ApJ, 137, 401
Raveendran, A. V. 1989, MNRAS, 238, 945
Savage, B. D., & Sembach, K. R. 1996, ARA&A, 34, 279
Smith, V. V., Lambert, D. L., & Nissen, P. E. 1993, ApJ, 408, 262
Sneden, C., Kraft, R. P., Prosser, C. F., & Langer, G. E. 1992, AJ, 104, 2121
Sturenburg, S. 1993, A&A, 277, 139
Tull, R. G., MacQueen, P. J., Sneden, C., & Lambert, D. L. 1995, PASP, 107, 251
Van Winckel, H., Mathis, J. S., & Waelkens, C. 1992, Nature, 356, 500
Van Winckel, H., Waelkens, C., & Waters, L. B. F. M. 1995, A&A, 293, L25
Venn, K. A., & Lambert, D. L. 1990, ApJ, 363, 234
Waelkens, C., Van Wickel, H., Trams, N. R., & Waters, L. B. F. M. 1992, A&A, 256, L15
Wahlgren, G. M. 1992, AJ, 104, 1174
Wasson, J. T. 1985, Meteorites: Their Record of Early Solar System History (New York: Freeman)
Waters, L. B. F. M., Trams, N. R., & Waelkens, C. 1992, A&A, 262, L37
Zsoldos, E. 1991, Ap&SS, 181, 203